J. Plasma Physics (1997), *vol.* 58, *part* 3, *pp.* 385–394. Printed in the United Kingdom

© 1997 Cambridge University Press

Instabilities of intense shock waves in monatomic gases

R. ANNOU[1] and B. FERHAT[2]

[1] Physics Department, Indian Institute of Technology, New Delhi 110016, India
[2] Observatoire de Paris, 92195 Meudon Cedex, France

(Received 10 February 1995 and in revised form 22 August 1996)

A wave-front distortion of strong shock waves in gases for particular Mach numbers M has been repeatedly noted. We propose two approaches according to which there is a threshold Mach number above which the instability occurs; this Mach number is related to the unperturbed gas pressure P_1. The first approach is macroscopic, and takes account of radiation; the second is microscopic, and takes account of radiation, electron diffusion to the walls of the shock tube and the non-equilibrium relaxation processes. A mechanism of four reactions is proposed. A nonlinear differential equation system is established. The latter becomes unstable for critical values of the Mach number.

1. Introduction

When a shock wave (SW) is formed in a shock tube, its front is expected to be plane as a consequence of the classical equations (Zeldovich and Raizer 1966; Laudau and Lifshitz 1979; Jaumotte 1973). However, it has been repeatedly noted that the SW becomes unstable at particular Mach numbers M and unperturbed gas pressure P_1. This phenomenon was noted for the first time in 1954 by Shreffler and Christian. Thereafter, many authors have studied it, and many criteria for stability have been proposed (Griffiths *et al.* 1975; Glass and Liu 1978; Ferhat 1979; Tumakaev *et al.* 1980; Ryazin 1980; Aslam and Ryazin 1984; Egorushkin *et al.* 1990). In the previous work, the following results have been reported: radiation, electron diffusion to the walls of the shock tube and non-equilibrium relaxation processes are the most important parameters suspected to be the cause of the instability. Moreover, the phenomenon is of a threshold type. However, in the available literature there is no mathematical model that includes all these parameters and gives the conditions for the instability to occur for a given pair of Mach number and unperturbed gas pressure (M, P_1). In this paper we present two approaches.

The first approach is a macroscopic one, consisting of a model called the 'BB-layer model' that takes account of radiation; when the SW is strong enough, it ionizes the gas through which it propagates, and for particular Mach numbers the radiation coming from behind the front is absorbed by the latter, which behaves like a black body. This Mach number is related to the unperturbed gas pressure P_1 through a law derived here.

The second approach is a microscopic one, consisting of a trimolecular model that includes in a coherent manner radiation, electron diffusion to the walls of the shock tube and non-equilibrium relaxation processes. Indeed, the ultimate

https://doi.org/10.1017/S0022377897006016 Published online by Cambridge University Press

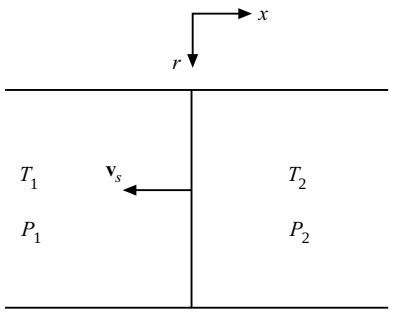


Figure 1. The front is a discontinuity propagating from left to right and dividing the gas into two compartments, namely unperturbed gas (T_1, P_1) and shock-heated gas (T_2, P_2).

action of a strong SW is gas ionization, which can be affected by radiation and particle escape to the walls (Biberman *et al.* 1979). Therefore we should study the microscopic structure of the front itself, which is a transition layer connecting the unperturbed gas defined by (T_1, P_1) and the ionized or the shock-heated gas defined by (T_2, P_2) (see Fig. 1). Thus we propose an ionization mechanism that gives rise to a nonlinear differential system. The analysis of the above-mentioned system proves the existence of critical Mach numbers and distortion of the front beyond these numbers.

2. Macroscopic approach: 'BB-layer' model

When the amplitude of a shock wave (SW) is high, it ionizes the gas through which it propagates. The latter emits radiation that is absorbed by the cold gas in front of the SW. Thus the gas is heated to a temperature T' (see Fig. 2). Accordingly, the compression propagates in a preheated gas, and the temperature T_f is therefore greater than evaluated in the non-heating case. This temperature will decrease to T_2 by means of radiation emission. The front is the layer where the transition from the state (T_1, P_1) to the state (T_2, P_2) has occurred, and δ^* is a layer where the temperature has a peak. It can be taken as a hydrodynamic transition zone.

The homogeneous plasma produced behind the front, i.e. the radiating zone, is a black body, emitting at a temperature T_2 several frequencies according to Planck's function, the most prominent frequencies being around the peak of the spectrum ($\approx 2.82\, k_B T_2/\hbar$). However, in the present model we assume radiation coming from behind the front as a set of photons having the same energy and corresponding to the centre of gravity of the spectrum. This energy may be expanded in a series (Gillet *et al.* 1989)

$$\bar{\omega} = \omega_a + \frac{k_B T^*}{\hbar} + 3\left(\frac{k_B T^*}{\hbar}\right)^2 \frac{1}{\omega_a} + \dots, \tag{1}$$

where T^* is a parameter depending on T_2, and ω_a is the frequency below which the frequencies in the spectrum are not effective.

The parameters of the gas in the front are evaluated at high Mach number M by taking into account the radiative flux $\mathbf{s}$ in the conservation equations. We get

$$\left(\frac{T_f}{T_1}\right)_\infty = \frac{\gamma^* M^2}{4}, \qquad \left(\frac{T_f}{T_2}\right)_\infty = 2.5, \tag{2}$$

where γ^* is the specific-heat ratio in the front.

https://doi.org/10.1017/S0022377897006016 Published online by Cambridge University Press

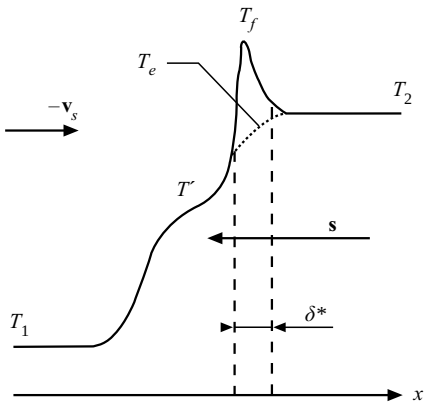


Figure 2. Illustration of the propagation sense of the radiation flux **s** and the unperturbed gas (T_1, P_1) with respect to the front.

The δ^* layer in the front is a plasma layer that can absorb radiation coming from the radiating zone for particular Mach numbers. Hence it becomes optically thick and behaves like a black body (Ryazin and Ferhat 1980). This happens for a transition frequency $\omega_{\rm tr}$ when the optical length $a_\omega \delta^*$ is equal to unity, where a_ω is the spectral linear absorption coefficient. To calculate $\omega_{\rm tr}$, we use the spectral linear absorption coefficient already evaluated by Hughes (1975), but changing the classically averaged Gaunt factor $\bar{g}_c$ by the the Greene-averaged Gaunt factor $\bar{g}_B$, since the temperature is high. We find for $\omega_{\rm tr}$,

$$1 = \left(\frac{n_e n_i Z^2 e^6}{6\pi\hbar\epsilon_0^3 c m_e}\right)\left(\frac{m_e}{2\pi k_B T_e}\right)^{1/2} e^{\hbar\omega_{\rm tr}/k_B T_e} K_0\left(\frac{\hbar\omega_{\rm tr}}{2k_B T_e}\right)\frac{e^{\hbar\omega_{\rm tr}/k_B T_e}-1}{\omega_{\rm tr}^3 \mu^3(\omega_{\rm tr})}\delta^*, \tag{3}$$

where n_e, n_i, Z, μ, k_B and $K_0(X)$ are the electron density, ion density, charge, refractive index, Boltzmann's constant and McDonald's function.

Now that all the parameters have been defined, let us develop the 'BB-layer' model. This model is based on the following idea: we claim that, for a given unperturbed gas pressure P_1, there is a particular Mach number $M_{\rm tr}$ above which the radiation coming from behind the front is absorbed by the δ^* layer. This means that for this Mach number the frequency $\bar{\omega}$ of photons coming from the shock-ionized zone corresponds to the transition frequency $\omega_{\rm tr}$ of the δ^* layer, which behaves like a black body at a temperature T_f. This statement can be formulated as follows:

$$\bar{\omega}(M_{\rm tr}) = \omega_{\rm tr}(M_{\rm tr}). \tag{4}$$

Equation (4) constitutes a stability criterion that can be developed to prove the existence of such Mach numbers and relate them to experimental conditions. Therefore we model the δ^* layer by assuming the temperature to be constant through it. The ion and electron temperatures are different because of the mass difference. We assume too that $T_e \approx T_2$ and $T_i \approx T_f$; δ^* and μ are taken as constant.

Using (1)–(4) but keeping only the first term in (1), we finally find

$$M_{\rm tr}^2 \exp\left[\frac{-10.12}{k_B T_1 \gamma^*} I\left(\frac{1}{M_{\rm tr}^2}\right)\right] = \frac{K}{P_1}, \tag{5}$$

https://doi.org/10.1017/S0022377897006016 Published online by Cambridge University Press

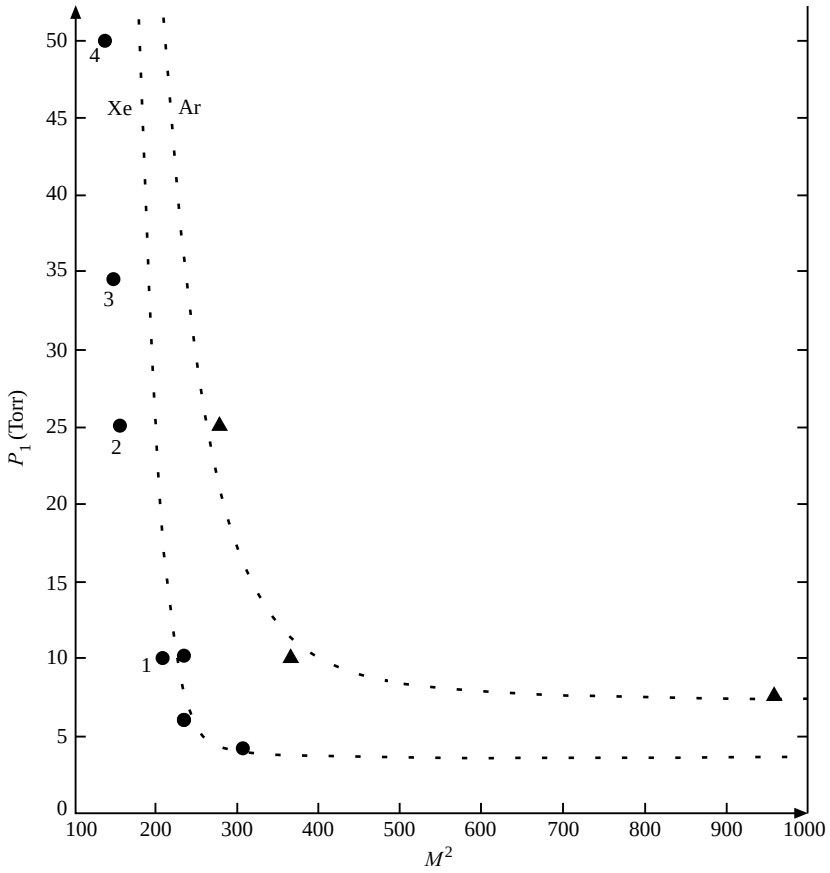


Figure 3. Theoretical curves (dotted) for argon and xenon together with experimental points (▲, Ar; ●, Xe). Points 1–4 were obtained by extrapolation (Ferhat 1979), and are expected to be closer to the theoretical curve.

where K is a constant and I the ionization potential. Moreover, by including a suitable coefficient, we get, for $T_1 = 300$ K and $\gamma^* = 1.25$,

$$P_1 - a_2 = \frac{K}{M_{\rm tr}^2 + a_1} \exp\left(\frac{A}{M_{\rm tr}^2 + a_1}\right). \tag{6}$$

For argon (Ar), $A = 4948.25$, $a_1 = 300$, $a_2 = 7.5$ Torr and $K = 1.5$ Torr; for xenon (Xe), $A = 3892.13$, $a_1 = 66.66$, $a_2 = 3.68$ Torr and $K = 0.0032$ Torr.

The theoretical curve fits the experimental data well (see Fig. 3). These transition Mach numbers found in (6) correspond to an instability. In effect, since the temperature is high, radiation free energy should be added to the free energy of the plasma within the δ^* layer (Bazarov 1990). Accordingly, the specific heat is $(c_p)_\infty = dT^3 + d'T^6$, where $d = 4V(\sigma + \frac{1}{3}\nu R)$ and $d' = 16V^2\sigma^2/9\nu R$, and σ, ν, R and V are respectively Stephan's constant, the mole number, the perfect-gas constant and the volume. So, we can expand the thermometric conductivity in a power series in the temperature:

$$(\chi)_\infty = \frac{T^{-5}}{d'} - \frac{d}{d'} T^{-8}.$$

https://doi.org/10.1017/S0022377897006016 Published online by Cambridge University Press

Then the plasma in the layer is a medium with a thermometric conductivity written as $\chi = a^* T^n$, where $n \leqslant -2$.

This leads to an instability whenever the front absorbs the radiation coming from the shock-heated zone. To prove this, let us assume that at $t = 0$ the heat $Q/\rho C_p$ per unit area concentrated in the plane $x = 0$ with $T = 0$ elsewhere, where ρ is density, is absorbed (see Zeldovich and Raizer 1966). The dimensionless heat-conduction equation

$$(2+n)\frac{d}{d\xi}\left(f^n \frac{dt}{d\xi}\right) + \xi \frac{df}{d\xi} + f = 0, \tag{7}$$

where

$$\xi = \frac{x}{(a^* t Q^n)^{1/(n+2)}} \qquad T = \left(\frac{Q^2}{a^* t}\right)^{1/(n+2)} f(\xi),$$

and t is time, leads to

$$f(\xi) = \left[\frac{n}{2(n+2)}(\xi_0^2 - \xi^2)\right]^{1/n}.$$

The f function is normalized to unity as a result of energy conservation. However, calculation gives

$$\int_{-\infty}^{\infty} f(\xi)\, d\xi = \lim_{\xi_0 \to +\infty} \left[\frac{n}{2(n+2)}\right]^{1/n} B\left(1 + \frac{1}{n}, \frac{1}{2}\right) \xi_0^{1+2/n} \to \infty, \tag{8}$$

where $B(x, y)$ is the beta function. Since $n \leqslant -2$, the integral diverges instead of being equal to unity. This divergence is interpreted as being related to an instability. Physically, this may correspond to an infinite heat propagation celerity.

3. Microscopic approach

In Sec. 2 we have seen that, for particular Mach numbers, radiation is absorbed. However, to understand well how the gas is ionized, how the instability occurs, and how radiation, electron diffusion and non-equilibrium processes are responsible for that, we shall go further inside the structure. For this purpose, we define a mechanism of four reactions that can explain the front bifurcation. This set of reactions is not exhaustive, but is sufficient as a first step in formulating the instability of intense shock waves. It appears from the proposed mechanism that atoms are first excited by radiation coming from behind the front. This process is probable for resonance radiation. Since the pressure is high ($P_1 \approx 5$ Torr and $P_2 \approx 25$ atm), excited atoms are ionized by collisions with atoms (the reaction rate $k_1 \approx 10^{-9}$ cm^3 s^{-1}), this being a way to produce the 'priming electrons' responsible for the ionization of other excited atoms by electron impact ($k_3 \approx 10^{-8}$ cm^3 s^{-1}). Indeed to ionize Ar* excited to its first level we need just 4.3 eV instead of 15.8 eV. However, with such a high pressure, another channel becomes probable, namely three-body recombination ($k_2 \approx 10^{-30}$ cm^6 s^{-1}), which can be considered as a loss channel for electrons. In this paper recombination is assumed to occur in the neighbourhood of an excited atom. As far as our treatment is concerned, this reaction is very important, because it ensures that the mechanism satisfies the requirement of

https://doi.org/10.1017/S0022377897006016 Published online by Cambridge University Press

the HTL theorem stating that cooperative effects cannot exist in a system of two intermediate variables where processes are uni- or bimolecular only. The variables X and Y in this mechanism are the excited atoms and electrons, where electrons are diffusing to the walls with a coefficient D'_f. Choosing such a mechanism takes into account remarks by some authors. Biberman *et al.* (1979) have pointed out that deviation from ionization equilibrium can be affected by radiation and particle escape to the walls. Ryazin (1980) pointed out that the bifurcation can be the result of a density change in two steps in the front, with the second step being due to a fast ionization. Moreover, several factors can be taken into account, namely perturbations caused by the walls, a fast excited gas decay and the fact that the SW is propagating through a pre-excited gas.

The mechanism:

$$\left.\begin{array}{ll} \text{Photoexcitation} & \mathrm{A_t}+h\nu \overset{\alpha}{\rightarrow} \mathrm{A_t^*}, \\ \text{Ionizations by atom–excited-atom collision} & \mathrm{A_t}+\mathrm{A_t^*} \overset{k_1}{\rightarrow} \mathrm{A_t^+}+\mathrm{e^-}+\mathrm{A_t}, \\ \text{Three-body recombination} & \mathrm{A_t^+}+\mathrm{e^-}+\mathrm{A_t^*} \overset{k_2}{\rightarrow} \mathrm{A_t}+\mathrm{A_t^*}, \\ \text{Excited-atom ionization by electron impact} & \mathrm{A_t^*}+\mathrm{e^-} \overset{k_3}{\rightarrow} \mathrm{A_t^+}+2\mathrm{e^-} \end{array}\right\} \quad (9)$$

where α_1, k_1, k_2 and k_3 are the reaction rates. The mechanism can be modelled to give

$$\left.\begin{array}{r} \tilde{\mathrm{A}}+h\nu \overset{\alpha}{\rightarrow} \tilde{\mathrm{X}}, \\ \tilde{\mathrm{B}}+\tilde{\mathrm{X}} \overset{k_1}{\rightarrow} \mathrm{A^+}+\tilde{\mathrm{Y}}+\tilde{\mathrm{B}}, \\ \mathrm{A^+}+\tilde{\mathrm{X}}+\tilde{\mathrm{Y}} \overset{k_2}{\rightarrow} \tilde{\mathrm{C}}+\tilde{\mathrm{X}}, \\ \tilde{\mathrm{X}}+\tilde{\mathrm{Y}} \overset{k_3}{\rightarrow} \mathrm{A^+}+2\tilde{\mathrm{Y}}. \end{array}\right\} \quad (10)$$

Hence we obtain a nonlinear differential system (with $\partial/\partial\tau$ standing for non-equilibrium processes $D\nabla^2$ for electron escape and A for radiation)

$$\left.\begin{array}{l} \dfrac{\partial x}{\partial \tau} = A - BX - XY, \\ \dfrac{\partial Y}{\partial \tau} = BX - \delta XY^2 + XY - D\dfrac{\partial^2 Y}{\partial \eta^2}, \end{array}\right\} \quad A, B, D, \delta \in \mathbb{R}^+, \quad (11)$$

with von Neumann conditions stating that matter cannot diffuse through the wall:

$$\left.\frac{\partial X}{\partial \eta}\right|_{\eta=0} = \left.\frac{\partial X}{\partial \eta}\right|_{\eta=l} = 0 = \left.\frac{\partial Y}{\partial \eta}\right|_{\eta=0} = \left.\frac{\partial Y}{\partial \eta}\right|_{\eta=l},$$

where l is the tube dimension along the r axis, N is the unperturbed gas density, n_e is the electron density, n^* is the excited-atom density and v_s is the SW velocity. A' and B' are the densities of the $\tilde{\mathrm{A}}$ and $\tilde{\mathrm{B}}$ atoms, with A and B their dimensionless forms:

$$\tau = \left(t - \frac{x}{v_s}\right) k_3 N, \qquad X = \frac{n^*}{N}, \qquad Y = \frac{n_e}{N}, \qquad \eta = \frac{r}{l},$$

$$A = \frac{\alpha A'}{k_3 N^2}, \qquad B = \frac{k_1 B'}{k_3 N}.$$

https://doi.org/10.1017/S0022377897006016 Published online by Cambridge University Press

3.1. Stability analysis

Let us take $X-X_0=\zeta$ and $Y-Y_0=\chi$, where (X_0, Y_0) is the stationary and homogeneous solution of the system:

$$X_0=\frac{4A\delta}{[1+(1+4\delta B)^{1/2}]^2}, \qquad Y_0=\frac{1+(1+4\delta B)^{1/2}}{2\delta}, \tag{12}$$

After linearization, the above system becomes

$$\frac{\partial}{\partial\tau}\begin{pmatrix}\zeta\\ \chi\end{pmatrix}=\mathsf{L}\begin{pmatrix}\zeta\\ \chi\end{pmatrix}, \tag{13}$$

where

$$\mathsf{L}=\begin{pmatrix}-B-Y_0 & -X_0\\ 0 & -\dfrac{2A}{Y_0}+X_0-D\nabla^2\end{pmatrix} \tag{14}$$

is the Lyapunov matrix. From (14), we easily find that instability occurs for

$$B_m=\frac{1}{4\delta}\left[\left(\frac{2}{m^2\pi^2D}[(A^2\delta^2-A\delta Dm^2\pi^2)^{1/2}+A\delta]-1\right)^2-1\right]. \tag{15}$$

where m is an integer. Equation (15) is nothing but a relationship between a set of critical Mach numbers and the pressure P_1. Hence the existence of critical Mach numbers is proved. So, the gas is undergoing a transition from a thermodynamic state to another via an instability zone, since the intensity of the SW is increasing.

Let us take a simple example, wherein we assume the reaction rates to be constant with respect to temperature, except for $k_3\sim T^{1/2}\exp(-\Delta E/k_BT)$ (see Zeldovich and Raizer 1966). For $N\approx 10^{21}$ cm^{-3}, $B\delta\ll 1$ and $A\delta D\ll 1$. Hence (15) leads to

$$m^2D\approx A\delta, \tag{16}$$

Taking

$$T=\frac{\gamma^*}{4}T_1M^2, \qquad D=\frac{D_f'(M,N)}{l^2N^2k_3}=\frac{C_1(M,N)}{MN^2}\exp\left(\frac{4\,\Delta E}{\gamma^*k_BT_1M^2}\right),$$

$$A\delta=\frac{\alpha A'k_2}{k_3^2}=\frac{C_2}{M}\exp\left(\frac{8\,\Delta E}{\gamma^*k_BT_1M^2}\right),$$

(16) gives

$$\frac{N}{m}\approx\left[\frac{C_1(M_{\rm cr},N)}{C_2}\right]^{1/2}M_{\rm cr}^{1/2}\exp\left(\frac{4\,\Delta E}{\gamma^*T_1k_BM_{\rm cr}^2}\right). \tag{17}$$

Note that all of the excited atomic states relax together. The characteristic activation energies for exciting the atomic states appear to be about equal to the energies of the first excited states. This energy can be related to the ionization potential: $\Delta E\approx 0.3I$. Thus (17) gives

$$\frac{P_1}{m}\sim\Gamma(M_{\rm cr},N)M_{\rm cr}^{1/2}\exp\left(\frac{1.2I}{k_BT_1\gamma^*}\frac{1}{M_{\rm cr}^2}\right). \tag{18}$$

We should note the presence of the integer m, which indicates that for a given pressure one can find a set of critical Mach numbers in accordance with experiment; e.g., for Xe, $P_1=4$ Torr and $M=17.4$, 20.8 and 21.4 (see Ryazin 1980).

Equation (18) is just an attempt to show the possibility of deriving from a

https://doi.org/10.1017/S0022377897006016 Published online by Cambridge University Press

relaxation mechanism a relationship giving these critical Mach numbers and relating them to the experimental conditions. To improve the calculation, we have to find the explicit form of $\Gamma(M,N)$, and use the explicit forms of all the reaction rates with respect to temperature

$$(k_2 \propto T^{-9/2} \quad \text{and} \quad k_1 \propto T^{3/2}[1-(I-E^*)/k_B T]\, e^{-I/k_B T}).$$

3.2. Determination of the solution beyond the instability

The system was in a stable thermodynamic state for a given B, and is in a different state when crossing the critical point defined by B_c. To show the front distortion beyond this point, we derive the explicit form of the stationary solution bifurcating beyond B_c.

Hence we expand the operator L around B_c and find

$$\mathsf{L}_c\begin{pmatrix}\zeta\\ \chi\end{pmatrix} = \begin{pmatrix}\zeta\chi-(B-B_c)\,(-a\zeta+b\chi)\\ \delta X_0-\chi^2+\delta\zeta\chi^2+(2\delta Y_0-1)\,\zeta\chi-(B-B_c)\,c\chi\end{pmatrix}, \tag{19}$$

where a, b and c are constants. Since the corrections must be small in the vicinity of the bifurcation, we expand $\begin{pmatrix}\zeta\\ \chi\end{pmatrix}$ and $B-B_c$ with respect to an infinitesimal parameter ϵ:

$$\left.\begin{aligned}\begin{pmatrix}\zeta\\ \chi\end{pmatrix} &= \epsilon\begin{pmatrix}\zeta_0\\ \chi_0\end{pmatrix}+\epsilon^2\begin{pmatrix}\zeta_1\\ \chi_1\end{pmatrix}+\dots,\\ B-B_c &= \epsilon\gamma_1+\epsilon^2\gamma_2+\dots \quad .\end{aligned}\right\} \tag{20}$$

We find

$$\mathsf{L}_c\begin{pmatrix}\zeta_k\\ \chi_k\end{pmatrix} = \begin{pmatrix}\alpha_k\\ \beta_k\end{pmatrix}. \tag{21}$$

With the non-flux conditions $\zeta_{k,\eta}(0) = \zeta_{k,\eta}(1) = 0$ and $\chi_{k,\eta}(0) = \chi_{k,\eta}(1) = 0$, we find, as a first result,

$$\mathsf{L}_c\begin{pmatrix}\zeta_0\\ \chi_0\end{pmatrix} = 0.$$

This means that the vector $\begin{pmatrix}\zeta_0\\ \chi_0\end{pmatrix}$ is proportional to the eigenvector of L_c, i.e.

$$\begin{pmatrix}U_{mc}\\ V_{mc}\end{pmatrix} = \begin{pmatrix}C_1\\ C_2\end{pmatrix}\cos(m_c\pi\eta).$$

Thus we have to solve the system

$$\left.\begin{aligned}\mathsf{L}_c\phi &= \text{function},\\ \mathsf{L}_c\phi_0 &= 0,\end{aligned}\right\} \tag{22}$$

where L_c is not invertible. Thus, according to Fredholm's theorem, the system can have solutions if and only if the following orthogonality condition is satisfied:

$$\left\langle (U^*_{mc}, V^*_{mc})\begin{pmatrix}\alpha_k\\ \beta_k\end{pmatrix}\right\rangle = \int_0^1 (\alpha_k U^*_{mc}+\beta_k V^*_{mc})\, d\eta = 0, \tag{23}$$

or

$$\int_0^1 [C_1\alpha_k\cos(m_c\pi\eta)+C_2\beta_k\cos(m_c\pi\eta)]\, d\eta = 0,$$

where $\begin{pmatrix}U^*_{mc}\\ V^*_{mc}\end{pmatrix}$ is the eigenvector of L^*_c.

https://doi.org/10.1017/S0022377897006016 Published online by Cambridge University Press

Finally, we get

$$\left.\begin{aligned}\zeta &= \pm\left[\frac{B-B_c}{\gamma_2(m_c)}\right]^{1/2}\cos(m_c\pi\eta)+\frac{B-B_c}{\gamma_2(m_c)}\sum_0 P_m(m_c)\sin(m\pi\eta)\\ &= \zeta(m_c,\eta),\\ \chi &= \pm\left[\frac{B-B_c}{\gamma_2(m_c)}\right]^{1/2} C_2\cos(m_c\pi\eta)+\frac{B-B_c}{\gamma_2(m_c)}\sum_0 q_m(m_c)\sin(m\pi\eta)\\ &= \chi(m_c,\eta).\end{aligned}\right\} \tag{24}$$

Beyond the bifurcation, the system has an equal probability to be in two states. However, the most important result is that the densities are now dependent on spatial dimension, which means that the front is no longer plane and is now a different evolution-velocity surface. We might also say that the internal energy is transferred in kinetic form to particles non-uniformly along the η axis.

We should note that the transition between the stable thermodynamic state and the dissipative structure is a second-order phase transition, where $W \propto \pm[(B-B_c)/\gamma_2]^{1/2}$ is taken as the order parameter.

4. Conclusions

Two approaches have been proposed. The first is microscopic, consisting of a model that takes radiation into account. It has confirmed theoretically that instability of strong shock waves is a threshold phenomenon, corresponding to some particular Mach numbers. For example, for Ar, $P_1 = 7.6$ Torr and $M = 31$; for Xe, $P_1 = 4$ Torr and $M = 17.42$. We have derived a formula relating these Mach numbers to experimental conditions. Indeed, it is sufficient to choose a value for the unperturbed gas pressure P_1 and predict the Mach number beyond which instability occurs. For example, for Ar, $P_1 = 15$ Torr and $M \approx 18.0 \pm 1.2$; for Xe, $P_1 = 15$ Torr and $M \approx 14.7 \pm 0.9$. To avoid instability, P_1 should be small. It should also be noted that further experimental data sets are necessary to test the degree of accuracy of the suggested model.

The second approach is microscopic. It is based on a set of four atomic processes leading to ionization. Excited atoms and electrons are taken as the variables of the system. We have derived a nonlinear differential equation system that admits critical points. A formula has been derived relating the critical Mach numbers to experimental conditions. Beyond the instability, the front is no longer plane; above these Mach numbers, the front becomes distorted. The model also shows that for a given P_1 there is a set of critical Mach numbers. We should also note that to be able to relate $M_{\rm tr}$ to $M_{\rm cr}$ we should analyze (15) further.

Acknowledgement

R. A. wishes to thank Professor V. K. Tripathi for his interest in the work and for helpful advice.

https://doi.org/10.1017/S0022377897006016 Published online by Cambridge University Press

References

Aslam, S. and Ryazin, A. P. 1984 *Vestni. Mosk. Univ. Fiz.* **39**, 94.

Bazarov, I. 1990 *Thermodynamique*. Mir, Moscow.

Biberman, L. M., Vorobev, V. S. and Yakubov, I. I. 1979 *Usp. Fiz. Nauk* **128**, 233.

Egorushkin, S. A., Nekurovskii, M. L. and Uspenskii, U. S. 1990 *Dokl. Akad. Nauk SSSR* **313**, 39.

Ferhat, N. 1979 Candidate's dissertation, Moscow State University.

Gillet, D., Lafon, J.-P. J. and David, D. 1989 *Astron. Astrophys.* **220**, 185.

Glass, I. I. & Liu, W. S. 1978 *J. Fluid Mech.* **84**, 55.

Griffiths, R. W., Sandeman, R. J. and Hornung, H. G. 1975 *J. Phys. D: Appl. Phys.* **8**, 1681.

Hughes, T. P. 1975 *Plasmas and Laser Light*. Adam Hilger, Bristol.

Jaumotte, A. L. 1973 *Chocs et ondes de choc*, tome II. Masson, Paris.

Landau, L. and Lifshitz, E. 1979 *Fluid Mechanics*. Pergamon Press, Oxford.

Ryazin, A. P. 1980 *Pis'ma Zh. Tekh. Fiz.* **6**, 516.

Ryazin, A. P. and Ferhat, B. 1980 VINITI, Moscow.

Schreffler, R. and Christian, R. 1954 *Appl. Phys.* **25**, 327.

Tumakaev, G. K., Maslennikov, V. G. and Serova, E. V. 1980 *Pis'ma Zh. Tekh. Fiz.* **6**, 354.

Zeldovich, Ya. B. and Raizer, Yu. P. 1966 *Physics of Shock Waves and High Temperature Hydrodynamic Phenomena*. Academic Press, New York.

Appendix

$$\alpha_0 = 0, \qquad \alpha_1 = \zeta_0\chi_0 + a\gamma_1\zeta_0 - b\gamma_1\chi_0;$$

$$\beta_0 = 0, \qquad \beta_1 = (2\delta Y_0 - 1)\,\zeta_0\chi_0 + \delta X_0\chi_0^2 - c\gamma_1\chi_0;$$

$$\alpha_2 = \zeta_0\chi_1 + a\zeta_1\gamma_1 + a\gamma_2\zeta_0 - \gamma_1 b\chi_1 - b\gamma_2\chi_0 + \zeta_1\chi_0;$$

$$\beta_2 = 2\delta X_0\chi_0\chi_1 + \delta\zeta_0\chi_0^2 - \gamma_1 c\chi_1 - \gamma_2 c\chi_0 + (2\delta Y_0 - 1)\,(\zeta_0\chi_1 + \zeta_1\chi_0);$$

$$\frac{c_2}{c_1} \approx \frac{1}{X_0}\left[\frac{2A}{Y_0} - Y_0 - X_0 - B_c + m_c^2\pi^2 D\right];$$

$$I(m, m_c) = \frac{1}{m} - \frac{2m_c}{m^2 - 4m^2 c};$$

$$\gamma_2^2 = 2(cc_2^2 + bc_1c_2 - ac_1^2)^{-1}\left\{\sum_0 [c_1 q_m + c_1 c_2 p_m + 2\delta X_0 c_2^2 q_m + (2\delta Y_0 - 1)\,(c_1 c_2 q_m + c_2^2 p_m)]\, I(m, m_c) + \frac{3\delta c_1 c_2^3}{8}\right\};$$

$$p_m = -2I(m, m_c)\left(c_2 + \frac{4A\delta[\delta X_0 c_2^2 + c_2(2\delta Y_0 - 1)]}{[1 + (1 + 4\delta B_c)^{1/2}]^2}\right) \frac{2\delta[2\delta B_c + 1 + (1 + 4\delta B_c)^{1/2}]^{-1}}{m^2\pi^2 - \dfrac{4A\delta}{1 + 1(1 + 4\delta B_c)^{1/2}} + \dfrac{4A\delta}{[1 + (1 + 4\delta B_c)^{1/2}]^2}};$$

$$q_m = 2I(m, m_c)\frac{\delta X_0 c_2^2 + c_2(2Y_0\delta - 1)}{m^2\pi^2 - \dfrac{4A\delta}{1 + (1 + 4\delta B_c)^{1/2}} + \dfrac{4A\delta}{[1 + (1 + 4\delta B_c)^{1/2}]^2}}.$$

https://doi.org/10.1017/S0022377897006016 Published online by Cambridge University Press